ISTITUTO NAZIONALE DI FISICA NUCLEARE

Sezione di Milano

INFN/TC-93/02
8 Aprile 1993

L. Gini, A. Leone, D. Pedrini, L. Rossi, G. Volpini:

CRITICAL CURRENT MEASUREMENTS AT LASA LABORATORY

PACS.: 07.20.Mc

Servizio Documentazione
dei Laboratori Nazionali di Frascati

INFN – Istituto Nazionale di Fisica Nucleare
Sezione di Milano

INFN/TC–93/02
8 Aprile 1993

CRITICAL CURRENT MEASUREMENTS AT LASA LABORATORY

L. Gini A. Leone D. Pedrini L. Rossi G. Volpini
INFN – Sezione di Milano, Laboratorio LASA and Dipartimento di Fisica dell'Università di Milano, via fratelli Cervi 201, 20090 Segrate (MI), Italy

ABSTRACT

We describe the experimental apparatus and the measurement criteria for critical current measurements developed at LASA laboratory (Milan). The results of some measurements carried out on high current density Cu–NbTi wires to be used for inner and outer layers of LHC dipoles are presented. The system allows I_c measurements up to 1,200 A between 4.2 K and 2.2 K, in magnetic fields up to 13 T (4.2 K) or 15 T (2.2 K). The reproducibility of the I_c measurements is shown to be $\pm$ 1 A, while the total accuracy is better than 1%.

1 INTRODUCTION

Over the last few years INFN has funded a research activity in applied superconductivity at LASA laboratory. By the end of '93 we plan to be able to measure routinely critical currents up to 1,200 A on NbTi and Nb_3Sn wires as well as I_c up to 30,000 A on high–current NbTi cables, like those foreseen in the dipoles for the LHC accelerator. Our laboratory has a special commitment to LHC project and it collaborates already

with CERN in the activities concerning the prototypes of the high–field dipoles.

So far we have measured mainly the wires to be used for inner and outer layers of LHC dipoles. In this note we present the experimental technique and results of critical current measurements performed on NbTi wires.These wires have a diameter of 0.84 mm (outer layer) and 1.29 mm (inner layer), an α ratio (non–superconductor to superconductor volume ratio) between 1.6 and 1.8, and a nominal critical current of 450 A at 6 T (outer layer) and 600 A at 8 T (inner layer). Section 2 presents the experimental apparatus; some results are described in Section 3.

2 EXPERIMENTAL SETUP

2.1 Magnetic field

The magnetic field is provided by a superconducting solenoid, capable of a field in excess of 13 tesla at 4.2 K in a bore of 53 mm. The magnetic field inhomogeneity, defined as

$$\frac{B_{max} - B_{min}}{B_0}, \tag{1}$$

(where B_{max} and B_{min} are respectively the maximum and minimum field in the measuring zone and B_0 is the nominal field at the center of the magnet median plane) is less than 0.20% in the region occupied by the samples (R = 2.4 cm and $z \pm 2$ cm). A refrigerator, (usually indicated as λ–plate,) can be used to reduce the temperature down to about 2.17 K (liquid helium λ–point) in the lower part of the bath, which contains both the magnet and the sample, as the upper bath remains at athmospheric pressure and boiling liquid Helium temperature. This refrigerator is composed of an expansion chamber where liquid Helium is admitted through a needle valve. The pressure inside the chamber can be reduced at will by means of an external suction pump; as the liquid helium enters inside the chamber it expandes cooling the bath in contact with the λ–plate.

At T = 2.2 K the maximum field achievable is about 15 T. Magnetic field versus current ratio (0.13685 T/A) has been measured by means of a NMR probe.

2.2 Helium bath temperature

The liquid helium bath temperature is measured with a CGR sensor, calibrated by the manufacturer in the temperature range 1.2–300 K with a typical accuracy of $\pm$ 4 mK at 10 K. Since these probes are subject to magnetoresistive effect, we have calibrated them as a function of magnetic field at 4.2 K and 2.2 K. This calibration is periodically repeated to keep under control any ageing effect.

2.3 Voltage measurements

To measure the voltage drop along the measuring zone, a nanovoltmeter (mod. Keithley 182) has been adopted, with a maximum resolution of 1 nV. In our case the analog and digital filter are not employed, in order not to speed down too much the acquisition rate. The selected integration time is 100 ms. In practice in the measuring zone a measure each 300 mA has been taken. The signal distribution of a typical measurement in the flat zone, the so–called *baseline,* in which no voltage should appear, because the wire is still fully superconducting, is shown in fig. 1. The noise r.m.s. is found to be about

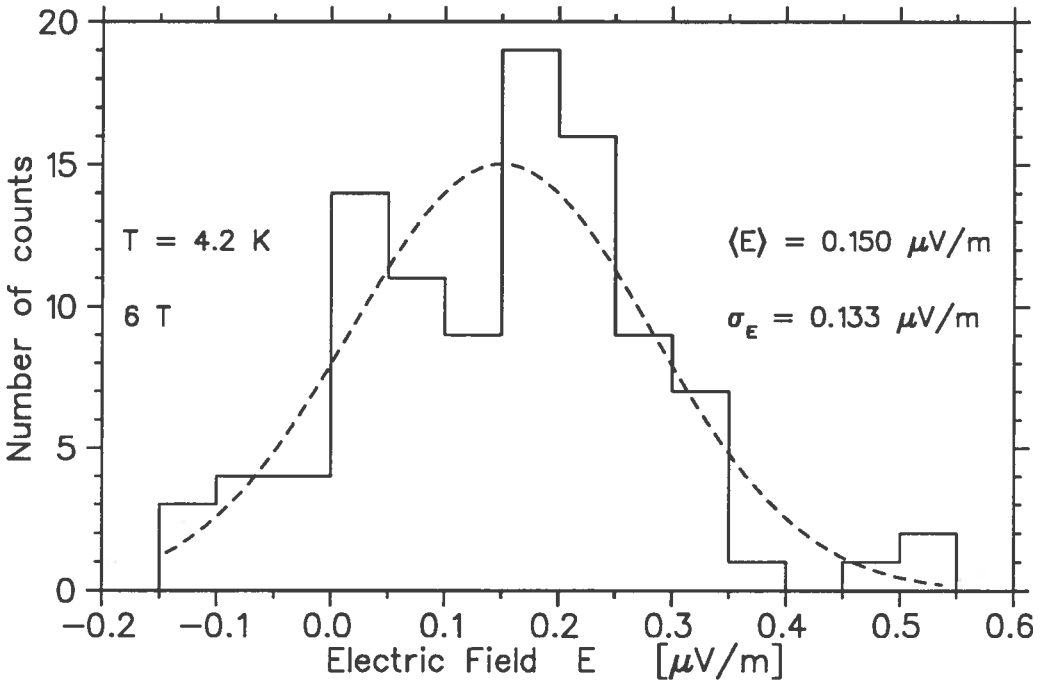

FIG. 1: Signal distribution in the flat part of the curve (full line). It has a guassian distribution with r.m.s. noise of $\sim$ 60 nV (the distance between the voltage being 42.5 cm in this case), as can be appreciated from the superimposed curve (dashed).

60 nV (the distance between volatge taps being 42.5 cm in this case); this value must be compared with an intrinsic r.m.s. noise of 18 nV of the instrument in the above configuration. The experimental noise is quite larger than the best value achievable with our instrument, but is largely sufficient for our purposes, at least in these first steps.

Since thermal electromotive forces (TEMF) can produce very large voltages compared to those we want to measure, care must be taken to eliminate any non–copper section in the circuit that connects the sample to the nanovoltmeter input. This is provided with a shielded low-thermal connector and cable, which anyway can not sustain low temperatures. Inside the magnet the voltage taps are formed by a couple of twisted copper wires which are connected, by means of lugs, to the outer cable. All

the connections are made by pression with screws. Only the connection to the sample is made with soft solder, since no other solution is pratically feasible.

The effect of residual TEMF can be as large as 1–2 μV. This value is quite stable and does not seem to drift during a measurement, so that its effect is completely negligible, when it is subtracted.

Values of critical current are calculated by considering data between 10 μV/m and 100 μV/m.

2.4 The current ramp

Often the I-V relation of a wire is determined either with a steady increasing current, with a $\frac{dI}{dt}$ in the order of some A/s, or in a stepwise fashion, changing the current of a finite amount, making a voltage measurement with stationary current, and so on.

The former method is simpler and faster but has some drawbacks, namely self-inductive spurious voltage, and inaccuracies due to the change of both current and voltage during the instrument integration time and to the delay between current and voltage measurement. This last phenomenon comes out when trigger to different instruments is not contemporary or integration time is different. All these problems become more severe with faster current ramp rate.

The latter method is slower but allows better results, since none of the above problems appears; moreover the integration time of the voltage measurement can be (in principle) as large as desired.

Our approach has been slightly different: we increase the current with a ramp instead of a stepwise fashion, but the $\frac{dI}{dt}$ is kept higher (in the order of 2-4 A/s) in the first part of curve (up to about the 60% of the expected I_c) which has small or no interest, and much slower afterwards (some hundreds of mA/s). Data are recorded only in the second part. This second part is large enough to allow us to calculate the baseline. The ramp rate is still low enough to make all the above–mentioned problems negligible.

The effect of self–inductance is estimated in the following way: the voltmeter is zeroed at the beginning of measurement with a stationary current of 1 A (this is done for reasons related to the power supply beahviour). When the current is growing at 2 A/s the signal is recorded, and it is found typically to be 300 nV. This ensures us that the self–inducted signal is negligible compared to the typical noise when the speed is decreased at 300 mA/s or even more at 100 mA/s.

Altough the approach described has proven to work well enough, we plan to proceed in the future with much faster current ramps (in the order of 5-20 A/s) because measurements presently performed may require quite a long time (1,000 s or even more for an I_c of 600 A.) From contacts with other laboratories (expecially with VAC [1]

and CERN [2] , where we had the opportunity to attend to some measurements) we have seen that the effect of the ramp rate is negligible ($\ll 1\%$). On the other hand, if very accurate measurements are required, it is definitely better to adopt a 'stepwise' current ramp rate.

2.5 Data acquisition

The measuring system is depicted in fig. 2. It is composed of a PC, that controls the whole process, a DC power supply that can provide up to 1,200 A, an HP-3852A data acquisition and control unit, an analog QDS (Quench Detection System) that triggers an electromechanical switch, and a Keithley-182 nanovoltmeter, which is described in the above section. Commands from PC to the current supply are sent through the HP-3852A. This control unit measures also the CGR resistance, voltage drops betweeen the warm terminals along the bus-bars (see § 2.6), the full voltage drops along the sample holder, the current flowing in the sample (through the signal coming from the internal DCCT of the power supply). Data are downloaded to the PC, stored into a file and printed on the screen. Voltage measurements are sent directly from the nanovoltmeter to the PC. All the communications between PC, data acquisition unit and nanovoltmeter take place through a GPIB protocol. The PC switches off the current when a voltage drop exceeding a given value (usually 50 μV) appears between the sample voltage taps. This method is not sufficient to guarantee the security of the system because of the following reasons:

- If a quench takes place outside the region between the voltage taps, this can not be identified until it has reached the sensitive zone. This extra time could be sufficient to damage the sample.
- The PC is in any case far too slow to react with the necessary speed to quench (these wires can carry 500-1,200 A in 5–8 T magnetic field). It makes about a measurement per second, while the current must be switched off within 100 ms from the beginning of quench.
- The system must be active also in case of a failure of PC.

For all these reasons an external QDS, completely independent of the PC, has been provided. The QDS measures the voltage drop along the whole sample and the bus bars. If a voltage larger than 15 mV is reached for more than 30 ms, an impulse is sent directly to the power supply that opens an electromechanical switch, sending to zero the current within 50 ms from the alarm. The above limits have been selected quite empirically so to suppress false alarms due to noise in the line, that can produce

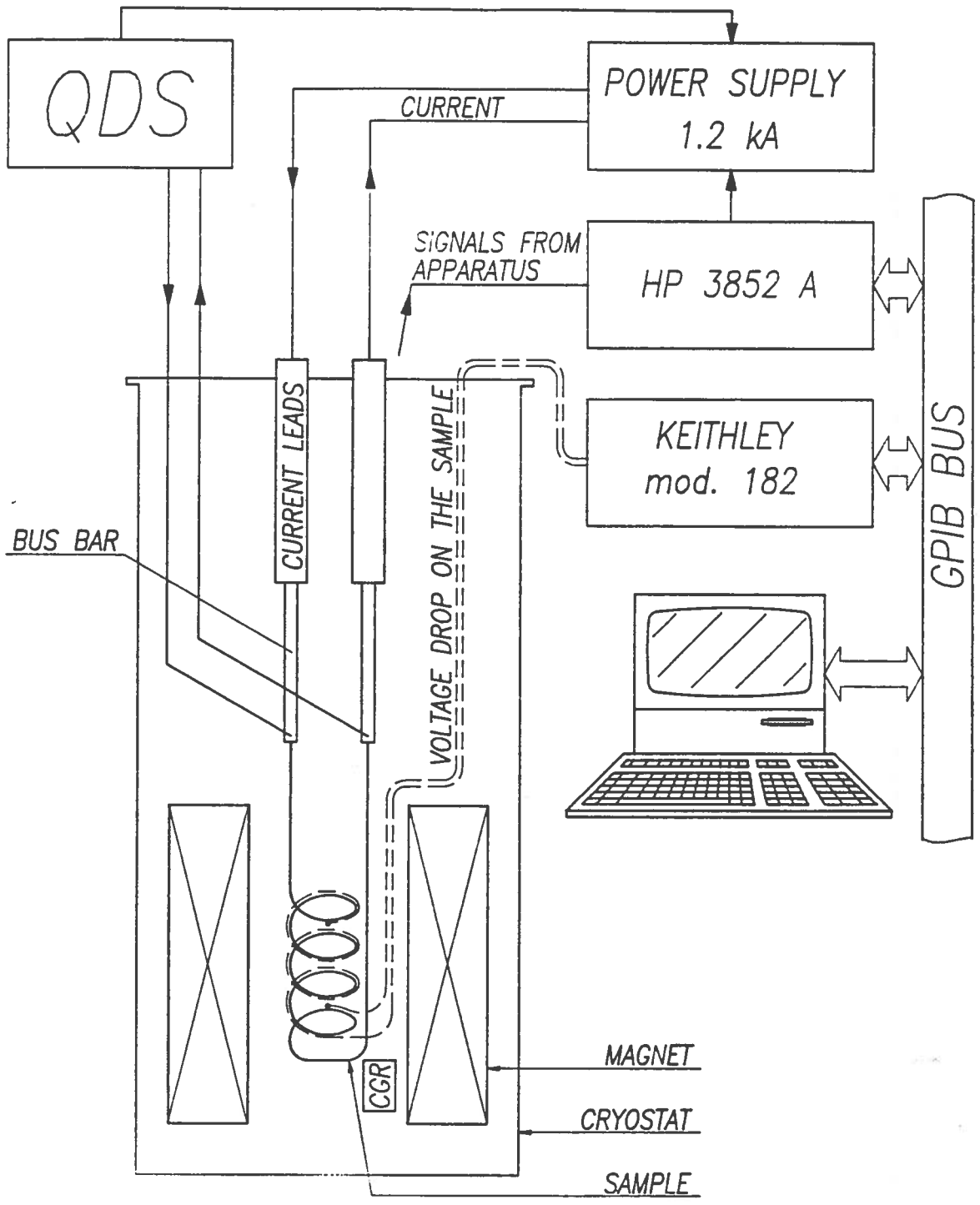

FIG. 2: Measuring apparatus lay-out.

large voltages for short times. They remain in any case largely sufficient to avoid any over-heating (and damage) to the sample.

2.6 Sample Holders

Two sample holders are currently being used, the first for current up to 600 A, and the second for current up to 1,200 A (see fig. 3). Their characteristic are quite similar.

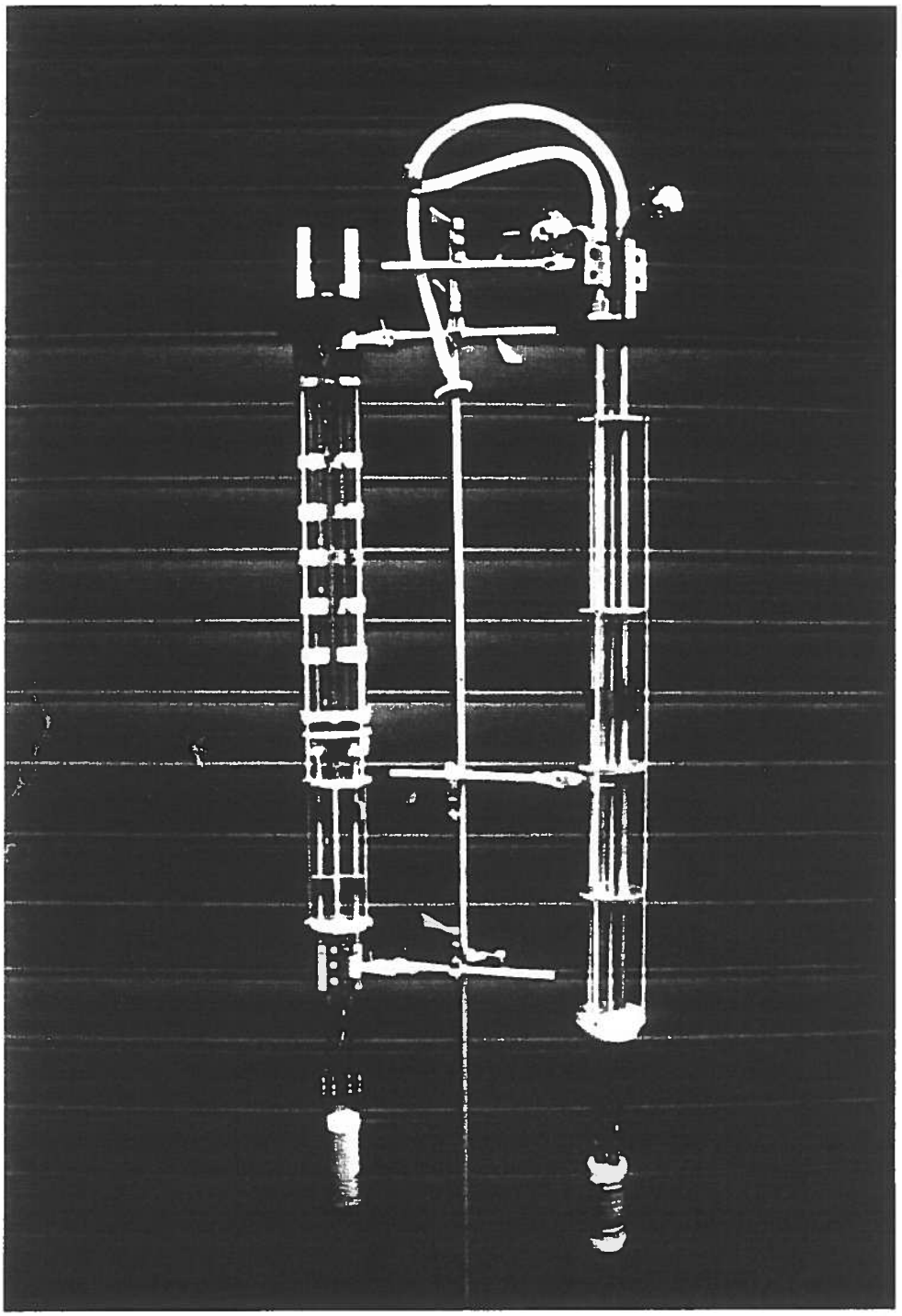

FIG. 3: The sample holders for 1,200 A (left) and for 600 A (right).

Their upper part is composed of two current leads, kept togheter by a G–11 or Tufnol flange. This flange is also used to fix the whole device to the magnet. The 600 A sample holder has standard forced gas cooled current leads provided by American Magnetics Corp. In the 1,200 A sample holder we have mounted currents leads from Cryogenics Consultants Ltd. These are formed of an upper section, composed by a bundle of hollow brass tubes, in such a way to offer the largest exchange surface to the helium gas, which is not in any case forced to flow inside. The lower section is formed by full copper rods, shunted by NbTi superconducting wires, which under normal operation carry the whole current. Also the bottom of the brass tubes composing the upper section is shunted with Nb_3Sn wires, to reduce heat dissipation due to Joule effect if the temperature is low enough.

The performance of both types of current leads is satisfactory; in the next sample holders we plan to adopt only forced gas cooled current leads. They are lighter, and therefore easier to handle, and have less heat flow inside liquid helium. Their only drawback is that the overpressure inside the helium cryostat may rise up to 50 mbar or more (in particular when operated at currents higher than maximum rated value, in this case 500 A) due to the fact that the gaseous helium exhaust can take place only through the current leads themselves. As a consequence, the liquid helium temperature may change significantly during a measurement. In any case this problem is not serious since the temperature is monitored continuously, as explained in § 2.2.

The current leads are connected to the sample under measurements by means of *bus-bars*. They are formed of a metallic rod to which some Nb_3Sn superconducting wires have been soldered. They carry current inside the liquid helium bath without any Joule dissipation. This is expecially important when the lower part of the bath, below the λ-plate, is cooled near the temperature of the superfluid helium. In this case, in fact, the total heat inlet must not exceed the λ-plate cooling power, about 1 W, and therefore all the heat sources have to be thoroughly minimized. For the same reason the metallic rod which sustains mechanically the Nb_3Sn and that carries current in case of a transition of Nb_3Sn, has a central section in stainless steel to reduce the thermal conductance between boiling helium and superfluid helium. In the 1,200 A current leads the contribution to heat flow from the stainless steel section is, for each bus-bur:

$$\frac{S}{L}\int_{2.17\mathrm{K}}^{4.22\mathrm{K}} dT\; k_{Steel}(T) \;=\; \frac{0.75\ \mathrm{cm}^2}{2.5\ \mathrm{cm}}\cdot 2\mathrm{mW/cm} \;\simeq\; 0.6\ \mathrm{mW}. \qquad (2)$$

If the whole bus–bar were in copper the heat input would be 10^3 times greater or even more. We must also take into account the thermal conductance of the copper used to stabilize the superconducting wires; in our case each bus-bar has three copper–stabilized Nb_3Sn wires, whose copper core section is 0.07 mm^2. The heat flow is

therefore

$$3 \cdot \frac{S}{L} \int_{2.17\mathrm{K}}^{4.22\mathrm{K}} dT\, k_{\mathrm{Cu}}(T) \;=\; \frac{0.0007\ \mathrm{cm}^2}{2.5\ \mathrm{cm}} \cdot 80\ \mathrm{W/cm} \;\simeq\; 70\ \mathrm{mW}. \qquad (3)$$

Since the section of stabilizing copper is of the same order as that of bronze matrix, we can neglect the contribution from the latter one.

To minimize direct thermal flow between the two baths a teflon cup closes the opening in the λ–plate. The closure is not tight beacuse a gas exhaust has to be present in case of magnet quench, and liquid helium must flow in the lower bath to compensate the λ–plate suction.

The sample is wound onto a groove carved in a G-11 barrel whose diameter is 45 (1,200 A sample holder) or 50 mm (600 A s. h.). The voltage taps are soldered on the wire at about 15 cm from current blocks, so to suppress any current redistribution voltage drop. The measuring zone between voltage taps is 42-44 cm. The voltage taps are anti-inductively wound. The CGR is located inside the G-11 barrel, in direct contact with liquid helium.

Some G–11 disk covered with aluminum tape, positioned along the current leads, act as radiation shield reducing the funnelling. Three vertical G–11 rods are fixed to the disk edges, thus allowing an easier insertion and removal of the sample holder from the magnet.

3 SAMPLES AND MEASUREMENTS

In this section we report, as example, the results of the measurements performed on two types of NbTi wires, produced by *Europa Metalli – LMI* (Italy) for the inner and outer layers of LHC dipoles. Their characteristics are reported in table 1.

	inner wire	outer wire
diameter	1.29 mm	0.84 mm
nominal α	1.6	1.8
nominal I_c at 4.2 K	600 A (8 T)	450 A (6T)
filament diameter	7.8 μm	
twist pitch	25 mm	

TABLE 1: Main characteristics of the wires.

Two specimens taken from each wire, one before and one after cabling, have been measured. This allows us to determine the degradation introduced by the cabling process.

I_c measurements have been performed at liquid helium (about 4.2 K) temperature for all the samples, and near superfluid helium temperature (2.17 K) for decabled inner

and outer wires. The cooling-down process from 4.2 K to 2.17 K takes 45 minutes so that we do not measure each sample at both temperatures. Data were analyzed by

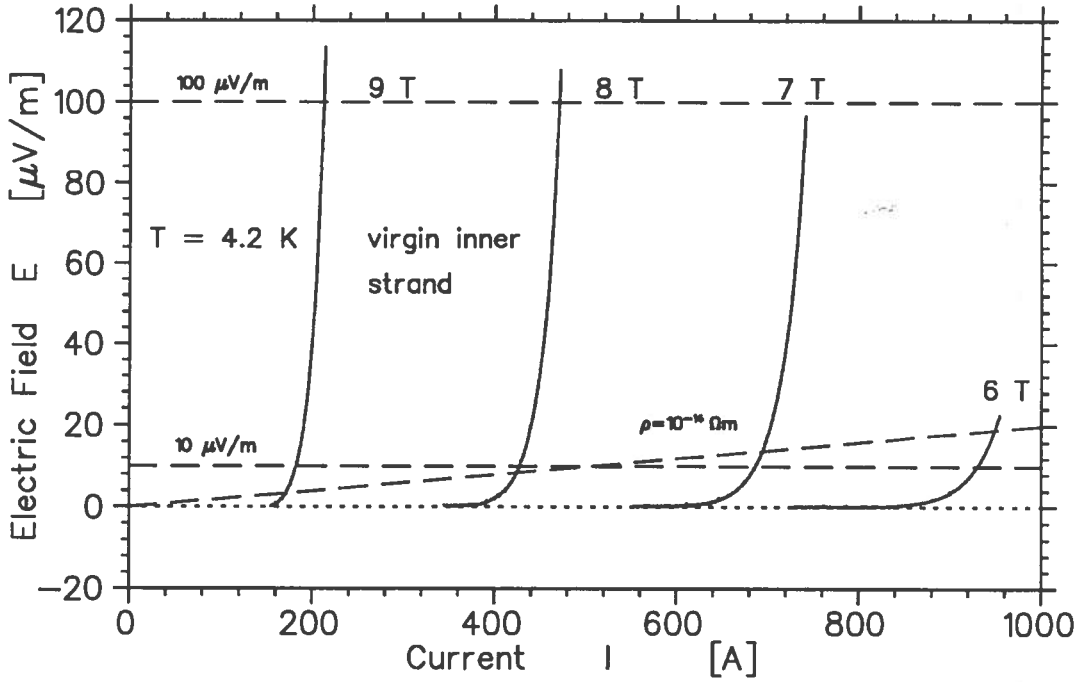

FIG. 4: Electric Field as a function of Current for virgin inner wire at 6, 7, 8 and 9 tesla, T = 4.2 K. The dashed lines represent the I_c criteria of 10 μV/m, 10^{-14} Ω·m, and 100 μV/m.

means of a computer programme which calculates the log E as a function of log I, evaluating directly the interpolated value of I_c, according to the criteria 10 μV/m, 10^{-14} Ω·m and 100 μV/m.

Points whose value is evidently influenced by some external factor can be excluded from interpolation by the operator. The results are reported in tab. 3, 4 and 5 for the inner wires and in tab. 6, 7 and 8 for the outer ones. Some measurements have been repeated for control, expecially at reference field, which is 8 (6) T at 4.2 K for the inner (outer) wire.

The liquid helium bath is never exactly at 4.22 K (the liquid helium boiling temperature at 1013 mbar), because of the overpressure due to the closed-circuit helium recuperation system. For this reason both values at bath temperature and values scaled at 4.22 K by means of Lubell's formulæ[3] have been reported.

The E–I curves are shown only in some cases, namely fig. 4 for inner virgin wire at 4.2 K, fig. 5 for outer decabled wire at 4.2 K and fig. 6 for outer decabled wire at 2.17 K. Only a measurements at each field has been reported, to make the picture clearer.

The log E as a function of log I graphs are shown in fig. 7 (inner wire) and fig. 8, 9 (outer wire). Even in this case only a measurements at each field has been reported. It

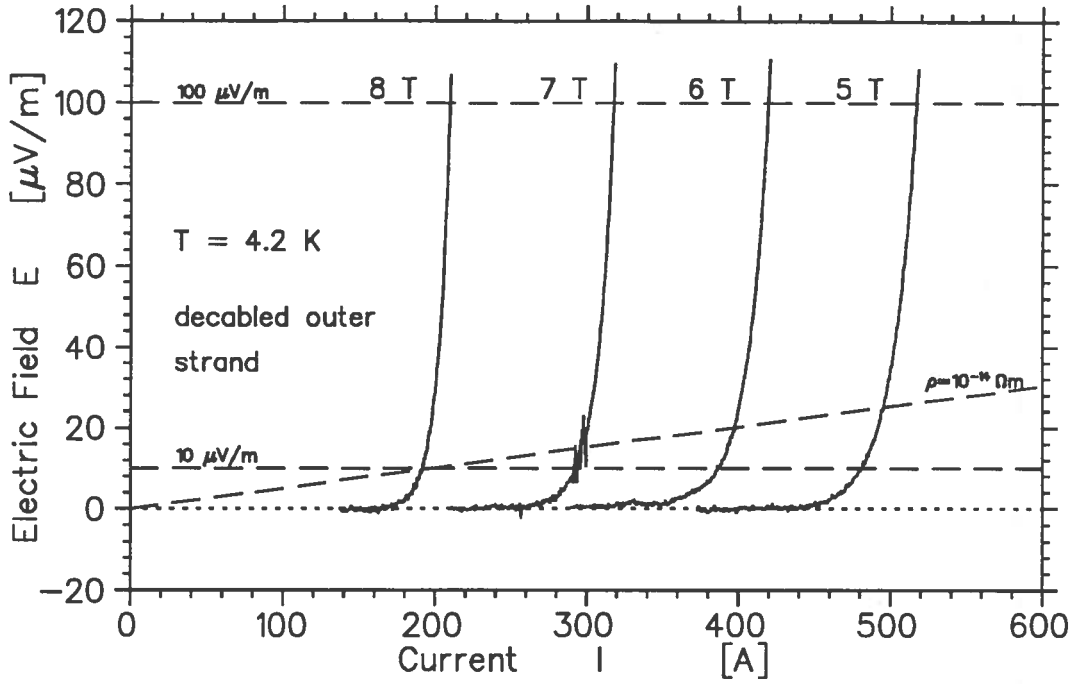

FIG. 5: Electric Field as a function of Current for decabled outer wire at 5, 6, 7 and 8 tesla, $T = 4.2$ K. The dashed lines represent the I_c criteria of 10 μV/m, 10^{-14} Ω·m, and 100 μV/m.

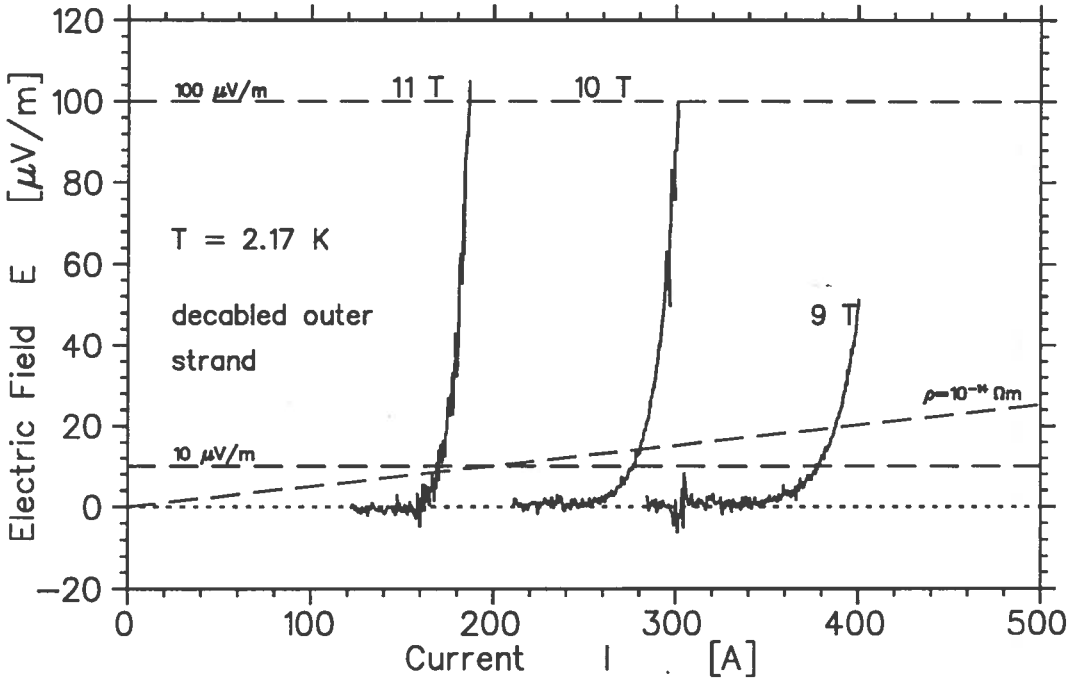

FIG. 6: Electric Field as a function of Current for decabled outer wire at 9, 10 and 11 tesla, $T = 2.17$ K. The dashed lines represent the I_c criteria of 10 μV/m, 10^{-14} Ω·m, and 100 μV/m.

can be seen that some points in the curve at 7 T for the outer wire were not considered, since they were influenced by a 'noise' appearing at I $\sim$ 300 A (see fig. 5), likely due

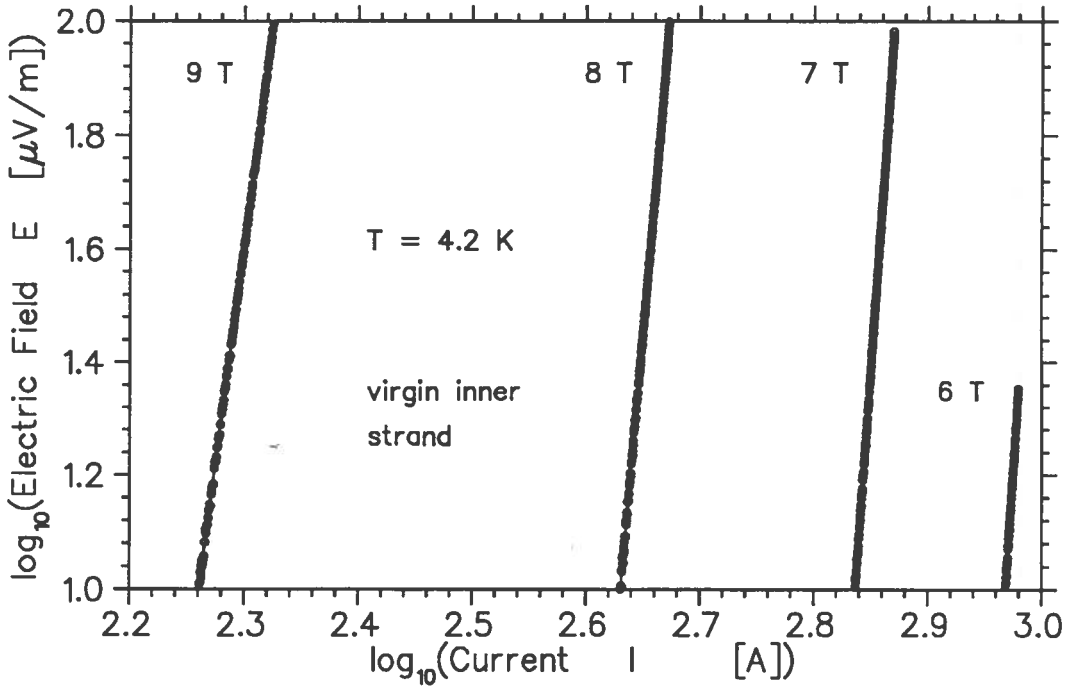

FIG. 7: Electric Field as a function of Current in bilogarithmic scale for virgin inner wire at 6, 7, 8 and 9 tesla, $T = 4.2$ K (compare fig. 4).

to the power supply.

Fig. 10 and 11 show the J_c (as calculated by taking into account the superconducting section only) as a function of B and n as a function of B at 4.22 K and 2.17 K for all

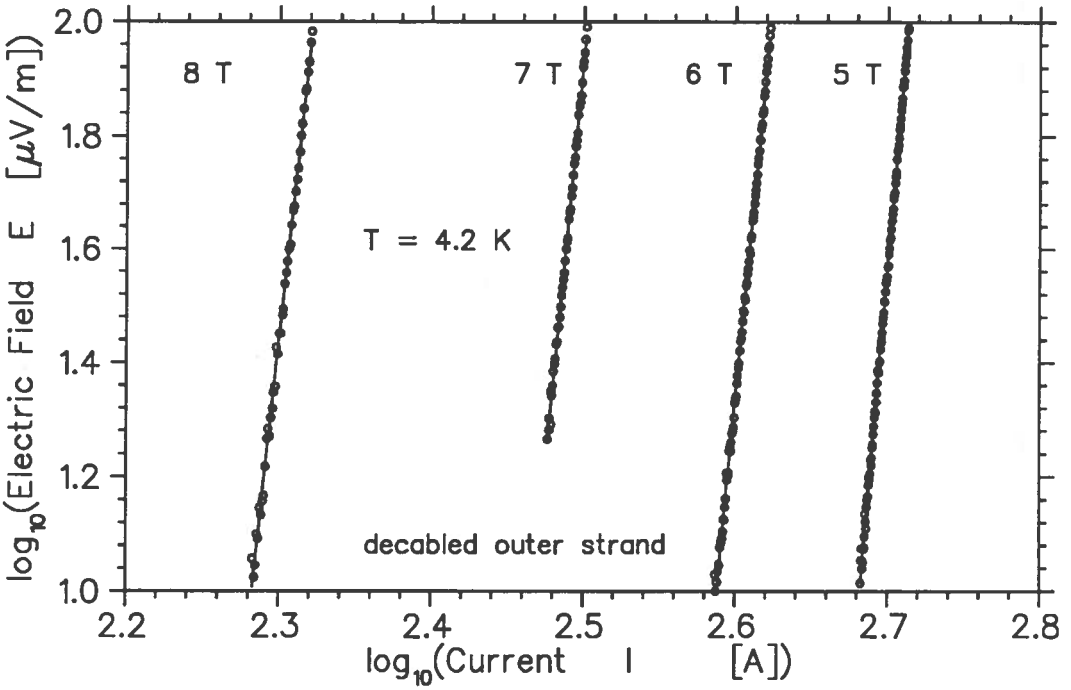

FIG. 8: Electric Field as a function of Current in bilogarithmic scale for decabled outer wire at 5, 6, 7 and 8 tesla, $T = 4.2$ K (compare fig. 5).

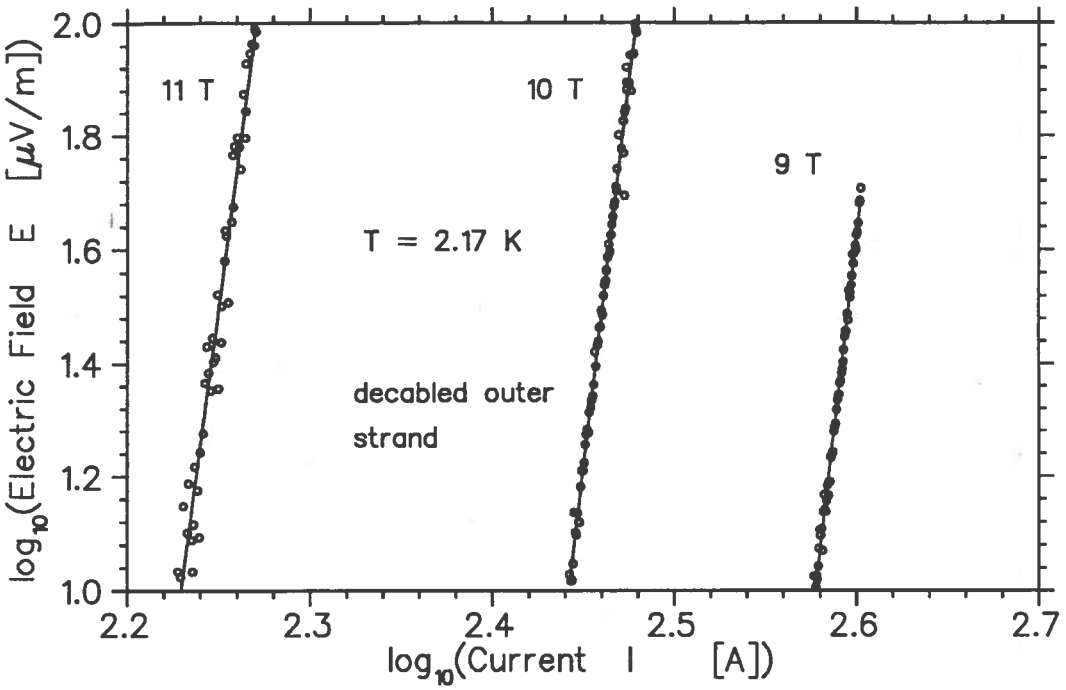

FIG. 9: Electric Field as a function of Current in bilogarithmic scale for decabled outer wire at 9, 10 and 11 tesla, $T = 2.17$ K (compare fig. 6).

the wires. Here we have considered the critical current values reduced at 4.22 K. The mean value for both I_c and n was taken in those cases where more measurements were made. If we extrapolate to zero J_c the $J_c(B)$ relation for both virgin and decabled wires (see tab. 2) we find values of B^*_{c2} in the range 9.94–9.96 T (4.22 K) and 12.63–

Wire	T [K]	B^*_{c2} [T]
Inner decabled	4.22	9.96
Inner decabled	2.17	12.67
Inner virgin	4.22	9.96
Outer decabled	4.22	9.94
Outer decabled	2.17	12.63
Outer virgin	4.22	9.96

TABLE 2: Values of B^*_{c2} found by extrapolating to zero the $J_c(B)$ relations shown in fig. 10.

12.67 T (2.17 K). These values can be compared with those calculated by means of Lubell's formulæ[3] 10.65 T (4.22 K) and 13.26 T (2.17 K). The difference between extrapolated and expected values is about –5%.

It is often interesting to extrapolate I_c measurements made at 4.22 K at lower temperatures; from our data on decabled wires we have found that the increase, passing from 4.22 to 2.17 K, of the magnetic field at which the same J_c is achieved is

about 2.71 T for decabled inner wire (4.2 K 8 T) and 2.82 T for decabled outer wire (4.2 K 6 T). These values can be compared with the change in B^*_{c2} between the same temperatures as calculated from Lubell's formulæ, 2.61 T.

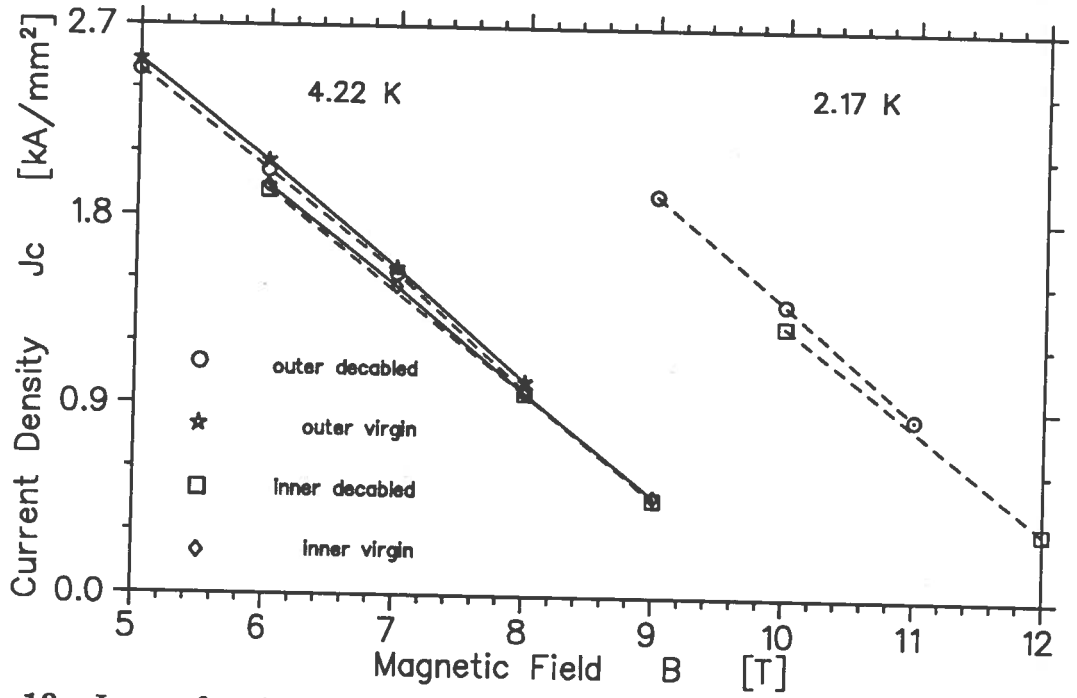

FIG. 10: J_c as a function of B at $T \sim 4.22$ K and 2.17 K. Dashed (full) lines connect measurements on the decabled (virgin) wire .

The degradation effect can be clearly shown in fig. 10. Its mean value is 2% and it does not appear to depend significantly on magnetic field. The α was evaluated by

	values at bath temperature		I_c [A] scaled at 4.22 K		
B [T]	I_c [A] (10 μV/m)	n	(10 μV/m)	(100 μV/m)	(10^{-14} Ω·m)
6	960.2	31.5	976.1	1050.1	997.6
7	722.6	29.5	738.2	798.1	748.2
8	467.0	23.6	481.4	530.7	480.5
8	467.9	23.8	482.3	531.3	481.4
8	468.2	23.9	482.6	531.4	481.7
9	227.6	15.5	239.4	277.7	227.4

TABLE 3: I_c of virgin inner wire at $T \sim 4.2$ K.

means of a chemical method. The values found are in agreement with those provided by the manufacturer.

Reproducibility of I_c measurements during the same thermal cycle is better than about 0.5% . A detail of three E vs. I curves at 6 T for the decabled sample is shown

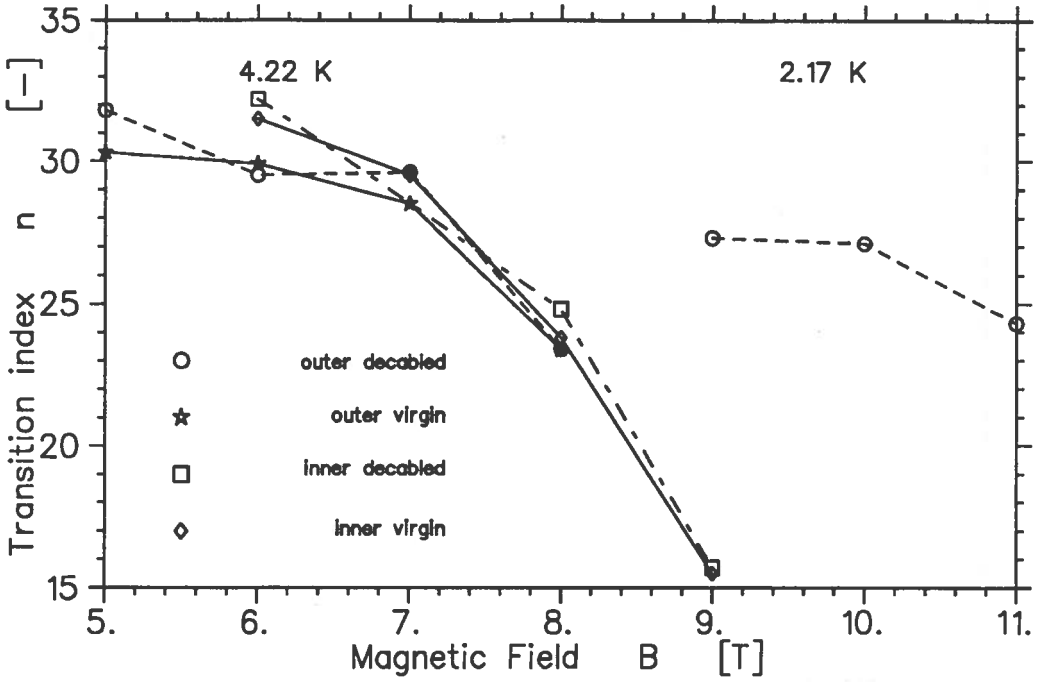

FIG. 11: n as a function of B at $T \sim 4.22$ K and 2.17 K. Dashed (full) lines connect measurements on the decabled (virgin) wire .

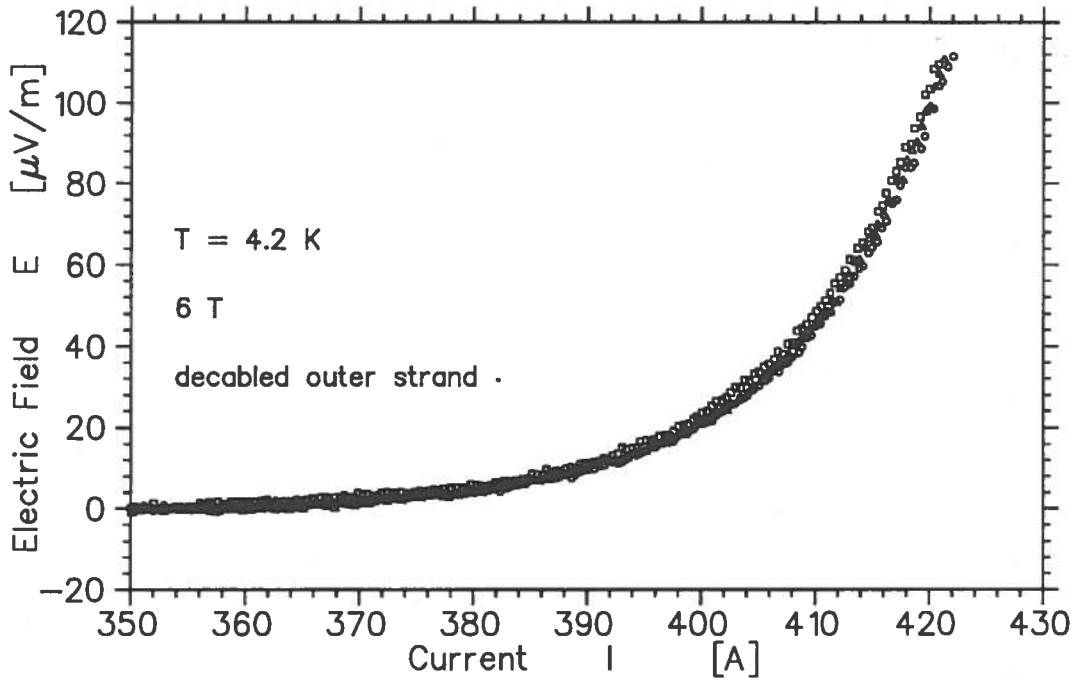

FIG. 12: A detail of three different E vs. I curves at 6 T for the decabled sample. The curves overlap within ± 1 A.

in fig. 12. All these curves were taken during the same thermal cycle, but between each other at least a measurement at another field was done. First curve (circles) is

	values at bath temperature		I_c [A] scaled at 4.22 K		
B [T]	I_c [A] (10 μV/m)	n	(10 μV/m)	(100 μV/m)	(10^{-14} Ω·m)
6	934.9	32.2	965.1	1036.6	985.4
8	458.2	24.9	480.7	527.3	479.8
8	457.3	24.7	479.8	526.7	478.9
9	215.1	15.7	232.5	269.2	220.6

TABLE 4: I_c of decabled inner wire at $T \sim 4.2$ K.

	I_c [A] values at 2.17 K			
B [T]	n	(10 μV/m)	(100 μV/m)	(10^{-14} Ω·m)
10	47.0	651.0	683.7	655.7
10	43.7	649.3	684.4	654.3
12	16.4	162.9	187.5	152.1
12	16.8	163.6	187.6	153.1

TABLE 5: I_c of decabled inner wire at T = 2.17 K.

the same as that shown in fig. 5.

The copper *RRR* (Residual Resistivity Ratio) of the decabled wire has been measured. This was done by letting a small current to flow inside the sample dived into liquid helium. The sample is then extracted from the liquid bath, and it warms up until it undergoes a resistive transition. Resistivity is measured again at room temperature to calculate the *RRR* ratio, which in our case turned out to be 76.2.

A standard NbTi reference wire, produced by NIST, was measured to make an absolute control of the performances of our system. The discrepancy between our results and those provided by NIST was less than 1%, between 2 and 8 T.

	values at bath temperature		I_c [A] scaled at 4.22 K		
B [T]	I_c [A] (10 μV/m)	n	(10 μV/m)	(100 μV/m)	(10^{-14} Ω·m)
5	489.5	30.3	501.3	540.9	516.7
6	396.7	29.9	407.5	440.1	417.0
6	396.5	29.9	407.3	439.9	416.8
6	396.1	30.0	406.9	439.4	416.3
7	298.1	28.5	307.7	333.6	311.8
8	193.0	23.4	200.9	221.6	199.9

TABLE 6: I_c of virgin outer wire at $T \sim 4.2$ K.

	values at bath temperature		I_c [A] scaled at 4.22 K		
B [T]	I_c [A] (10 μV/m)	n	(10 μV/m)	(100 μV/m)	(10^{-14} Ω·m)
5	481.1	31.8	491.9	528.8	506.3
6	389.2	29.9	399.2	431.2	408.7
6	389.5	30.1	399.5	431.3	409.0
6	387.4	28.4	397.4	431.0	407.4
7	293.9	29.6	303.1	328.3	308.0
8	190.2	21.3	191.8	213.6	191.4
8	191.7	25.5	193.3	211.5	193.0

TABLE 7: I_c of decabled outer wire at $T \sim 4.2$ K.

	I_c [A] values at 2.17 K			
B [T]	n	(10 μV/m)	(100 μV/m)	(10^{-14} Ω·m)
9	27.5	378.0	411.0	387.3
9	27.1	377.9	411.3	387.3
10	27.1	276.7	301.2	280.3
11	24.3	169.7	186.6	168.6
11	24.2	169.6	186.5	168.4

TABLE 8: I_c of decabled outer wire at T = 2.17 K.

4 CONCLUSIONS AND ACKNOWLEDGEMENTS

We have seen that I_c up to 1,200 A and n–index measurements on NbTi wires can be performed with an overall accuracy and reproducibility better than 1%, at $T = 4.22$ and 2.17 K and for magnetic fields ranging from 5 to 12 tesla. These measurements can now be performed routinely, even if we are planning some improvements to the test station that should make easier and faster (and possibly even more accurate) the whole measuring processus. In particular, since the power supply currently being used for these measurements shall be exploited later to power up a new superconducting magnet, we plan to develope a battery–operated power supply. This solution is cheaper than an ordinary power supply and should eliminate virtually any AC residual.

The authors wish to acknowledge gratefully prof. E. Acerbi for his suggestions and fruitful discussions, and Mr. G. Baccaglioni and Mr. G. C. Cartegni for the valuable technical assistance.

REFERENCES

(1) M. Thöner *priv. com.*

(2) L. Oberli *priv. com.*

(3) M. S. Lubell *"Empirical Scaling Laws for Critical Current and Critical Field for Commercial NbTi"* IEEE Trans. on Mag. **MAG–19,** 754 (1983)